13th Australasian Fluid Mechanics Conference
Monash University, Melbourne, Australia
13-18 December 1998

A COMPARISON OF TWO- AND THREE-DIMENSIONAL WAKES OF AN OSCILLATING CIRCULAR CYLINDER

Hugh M. Blackburn

Division of Building, Construction and Engineering
CSIRO, Highett, Victoria, AUSTRALIA

Department of Mechanical Engineering
Monash University, Clayton, Victoria, AUSTRALIA

ABSTRACT

Simulation results for two-dimensional and three-dimensional wakes of circular cylinders are compared at $Re = 265$, which is sufficiently high for the wake of a fixed cylinder to exhibit spatio-temporal chaos. Comparisons are made both for fixed cylinders and those in forced cross-flow oscillation. Assessments of the two-dimensionality of the three-dimensional wake flows are made on the basis of spanwise correlations of fluctuating forces and wake velocities, and also via Fourier analysis. Force coefficients from spanwise-averaged three-dimensional flows are compared with those for equivalent two-dimensional flows.

INTRODUCTION

Wake flows of prismatic bluff bodies are dominated by two-dimensional vortical structures known as the Kármán vortex street. It is true however that three-dimensional effects in the wake play a significant role in influencing cross-flow momentum transport (Cantwell & Coles 1983) and ultimately the strength and spanwise organisation of the main Kármán vortices. This has practical significance in the field of vortex-induced vibration, since increased spanwise organisation of fluctuating forces typically produces larger modal loads, hence larger vibration amplitudes than would otherwise exist.

Traditionally the 'three-dimensionality' of wakes produced by prismatic bluff bodies has been quantified via measures based on two-point cross-correlations of flow variables such as velocity, pressures, or fluctuating forces. An effect repeatedly observed is that at a given axial separation such correlations are enhanced when the body oscillates cross-flow at frequencies near the vortex shedding frequency (e.g. Novak & Tanaka 1975). Flow visualisations (Koopmann 1967) have also demonstrated that the Kármán vortices become more aligned with the body axis as cross-flow oscillation amplitudes increase.

These observations support the idea that wakes produced by oscillating bluff bodies are less dominated by three-dimensional effects than are those produced by the same body, but in fixed position. While this may be true, it has only been comparatively recently that the pervasive nature of end effects in determining the three-dimensionality of nominally two-dimensional flows has been fully appreciated (see e.g. Williamson 1989). The implication is that prior work concerned with quantification of three-dimensionality may have dealt primarily with phenomena determined by end effects rather than those inherent in the undisturbed flow. As a first step in rationalising the relative importance of inherently three-dimensional effects in completely two-dimensional geometries, the current work investigates three-dimensional flows in which end effects are absent, using direct numerical simulations which have domains that are periodic in the spanwise direction.

A related issue is the degree to which two-dimensional simulations give reliable information about flows which are three-dimensional at the same Re, particularly when a cross-flow oscillation is imposed. Here we compare the behaviour of spanwise-averaged three-dimensional flows with two-dimensional flows computed at the same Re, forced cross-flow oscillation amplitude and frequency ratio (based on the Strouhal frequency for the fixed cylinder).

PARAMETER VALUES

This work deals with turbulent three-dimensional wakes produced by a prismatic circular cylinder. With the advent of accurate methods for simulation and stability analysis of three-dimensional wakes it has become apparent that even for Reynolds numbers just above the onset of three-dimensionality, the wake of a circular cylinder exhibits spatio-temporal chaos (Henderson 1997). The chaotic fluctuations can be reproduced successfully by numerical simulations provided the number and wavelengths of modes or spanwise degrees of freedom are chosen with care. The Reynolds number used here is $Re = UD/\nu = 265$ where U is the frestream speed and D is the cylinder diameter. The spanwise length of the domain is $L_z = 13.12\,D$, with 72 Fourier modes (144 data

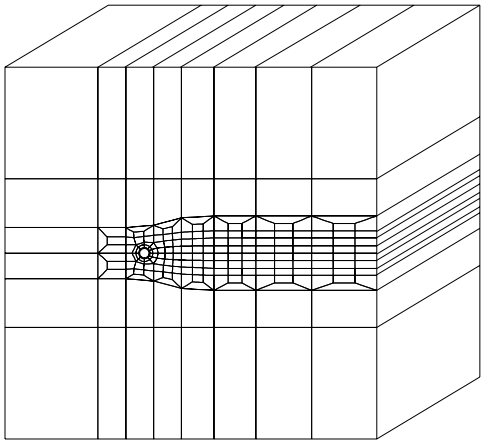

Figure 1: Computational mesh with 218 spectral/Fourier elements. The domain is $37.5\,D$ in streamwise extent, $40\,D$ in cross flow extent and $13.12\,D$ in spanwise extent.

planes) in the spanwise direction; these values are similar to those found adequate by Henderson for simulations of flow past a fixed cylinder at the same Reynolds number.

For the oscillating cylinder we have chosen an oscillation amplitude $A = y_{\max}/D = 0.25$ and frequency ratio $F = f_o/f_v = 0.8$, where f_o is the oscillation frequency and f_v is the vortex shedding ftequency for the fixed cylinder.

NUMERICAL METHOD

A spectral element/Fourier spatial discretisation has been used in conjunction with a second-order-accurate time-splitting scheme to solve the incompressible Navier–Stokes equations in an accelerating reference frame that moves with the cylinder axis. The method and previous applications have been described in Blackburn & Karniadakis (1993), Blackburn & Henderson (1996).

In the Fourier projection the three-dimensional field $\boldsymbol{u}$, which is assumed to be spatially periodic in the spanwise (z) direction, is projected onto a set of two-dimensional Fourier modes $\hat{\boldsymbol{u}}_k$

$$\hat{\boldsymbol{u}}_k(x,y,t) = \frac{1}{L_z}\int_0^{L_z} \boldsymbol{u}(x,y,z,t)\mathrm{e}^{-\mathrm{i}(2\pi/L_z)kz}\,\mathrm{d}z. \tag{1}$$

Introducing the notation $\beta_k = (2\pi/L_z)k$,

$$\tilde{\nabla} \equiv (\partial_x, \partial_y, \mathrm{i}\beta_k), \qquad \tilde{\nabla}^2 \equiv (\partial_x^2, \partial_y^2, -\beta_k^2),$$

the transformed incompressible Navier–Stokes equations for each Fourier mode k become

$$\frac{\partial \hat{\boldsymbol{u}}_k}{\partial t} + \widehat{\boldsymbol{N}(\boldsymbol{u})}_k = -\tilde{\nabla} P_k + \nu\tilde{\nabla}^2\hat{\boldsymbol{u}}_k. \tag{2}$$

Here $\widehat{\boldsymbol{N}(\boldsymbol{u})}_k$ represents the Fourier transform of the nonlinear product terms, which are computed in physical space to avoid formation of convolution sums. Another consequence of the Fourier decomposition is that the zeroth mode $\hat{\boldsymbol{u}}_0$ represents the spanwise-average field.

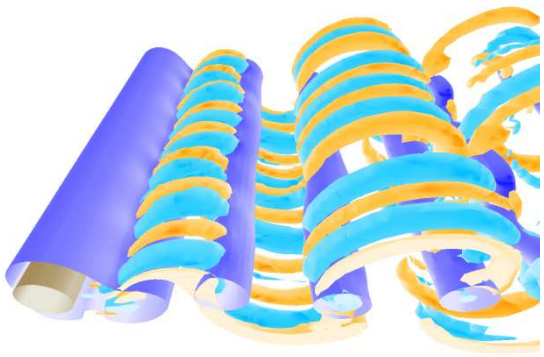

Figure 2: Flow past a fixed circular cylinder (left) at $Re = 265$. Isosurfaces of pressure (aligned mainly spanwise) and streamwise vorticity (aligned mainly streamwise).

The set of equations for each Fourier mode is an independent problem that can run concurrently, with interprocess communication needed only during the computation of the nonlinear terms $\widehat{\boldsymbol{N}(\boldsymbol{u})}_k$. The least restrictive implementation of the algorithm uses a distributed-memory programming model with explicit message passing. The three-dimensional computations presented here were run using six processors on a Fujitsu VPP-300 computer at the Australian National University Supercomputer Facility, with MPI as the message-passing kernel.

Mesh

The spectral element mesh is illustrated in figure 1. There are 218 elements, with 6th order tensor-product shape functions used for the (x,y) discretisation within each element. There are 144 planes or 72 complex Fourier modes of data in the spanwise direction, and in total the mesh has 1 149 120 node points.

RESULTS

Flow visualisation which illustrates the three-dimensionality of the flow past a fixed cylinder at $Re = 265$ is shown in figure 2. Streamwise-aligned structures are isosurfaces of streamwise vorticity, which contribute to the cross flow momentum transport in regions between the spanwise-aligned main rollers, which are represented by a pressure isosurface.

Measures of spanwise coherence

Figure 3 illustrates the effect of imposed cross flow oscillation on the three-dimensionality of the wake by showing contours of out-of-plane velocity on the wake centreline plane for a fixed and an oscillating cylinder.

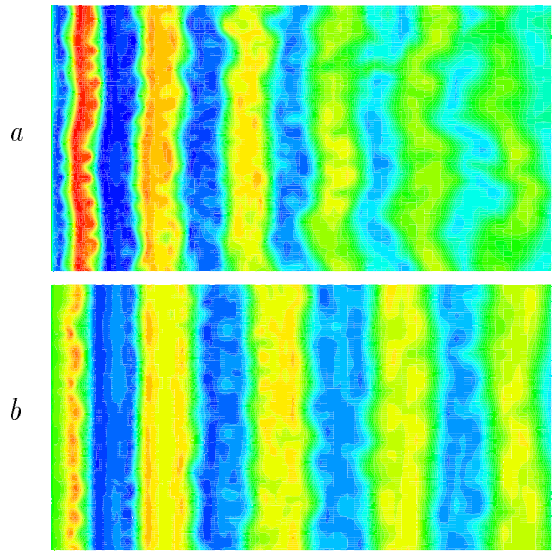

Figure 3: Contours of out-of-plane velocity (v) on the wake centre plane for a circular cylinder at $Re = 265$. (a): Cylinder fixed. (b): Cylinder forced to oscillate cross-flow at 78% of the Strouhal frequency for the fixed cylinder, $y_{\max}/D = 0.25$.

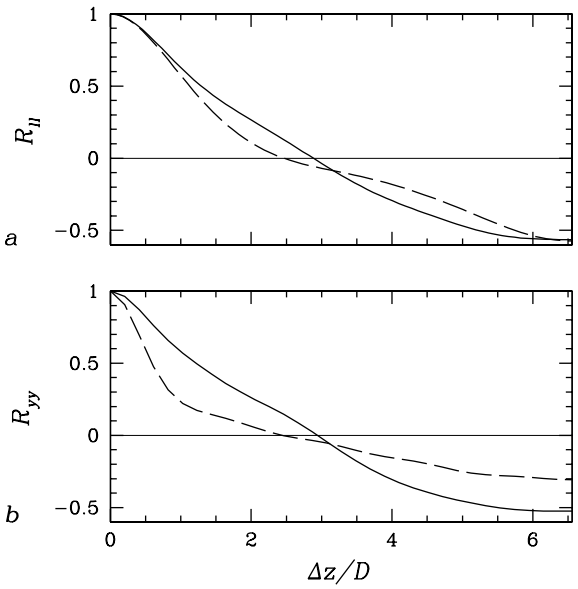

Figure 4: Comparison of spanwise autocorrelations for the fixed (– –) and oscillating (——) cylinders. Autocorrelations of (a), lift force; (b), out-of-plane velocity (v) on the centre plane, $20\,D$ downstream.

Visually the effect of oscillation is to provide increased spanwise correlation, both in the near and far wake.

The traditional way to assess spanwise organisation of such flows is through two-point spanwise autocorrelation functions of quantities such as pressure, force, or wake velocities. In figure 4, these are compared for lift force, and the out-of-plane velocity component (v) on the simulation centre plane, $20\,D$ downstream from the cylinder centre. Since the simulations are periodic in the spanwise direction, circular autocorrelation functions have been used. The effect of oscillation is to increase the correlations somewhat, although, in line with what might be expected from figure 3, the effect on the spanwise correlation of lift is not as marked as that on the wake velocities far downstream.

Another means to quantify three-dimensionality is based on the spanwise Fourier decomposition. The amount of kinetic energy in each mode k can be computed as

$$E_k = \frac{1}{2A}\rho \int_\Omega \hat{\boldsymbol{u}}_k \cdot \hat{\boldsymbol{u}}_k \, \mathrm{d}\Omega, \qquad (3)$$

where A is the area of the two-dimensional domain Ω. Time series of E_k for both the fixed and oscillating cylinder are presented in figure 5. In both cases, the energy in the $k = 0$ mode is dominant, with a value $E_0 \approx 0.5$ corresponding to the freestream speed $U = 1$. It can be seen that for the fixed cylinder (figure $5a$), the amount of energy in the modes $k \geq 1$ is greater than is the case for the oscillating cylinder, figure $5b$.

A measure of the two-dimensionality of the flow is given by the time-average of the energy in the higher Fourier modes normalised by the energy in the spanwise-average ($k = 0$) mode

$$R_d = \left\langle \sum_{k=1}^{N-1} E_k/E_0 \right\rangle. \qquad (4)$$

For the fixed cylinder, $R_d = 540 \times 10^{-6}$, while for the oscillating cylinder, $R_d = 295 \times 10^{-6}$. This confirms that the flow for the oscillating cylinder is more two-dimensional than for the fixed cylinder.

Three-dimensional vs. two-dimensional flow

While the values for R_d demonstrate that the three-dimensional wake of the oscillating cylinder is more two-dimensional than the three-dimensional wake of the fixed cylinder, the question remains: How much is the three-dimensional wake of the oscillating cylinder like the wake for an equivalent two-dimensional oscillating cylinder? We can make a start on answering the question by comparing global measures such as lift and drag coefficients C_l, C_d produced by the three-dimensional simulations against results for equivalent two-dimensional simulations.

Figure 6 shows two sets of coefficient of lift time series which compare results for the two-dimensional and three-dimensional flows. In figure $6a$, C_l values for the fixed cylinder are compared, and the timebase has been normalised using the vortex shedding period (its average value in the case of the three-dimensional flow). The magnitudes of C_l values are similar: the lower value for the three-dimensional flow reflects the lower spanwise coherence in that case.

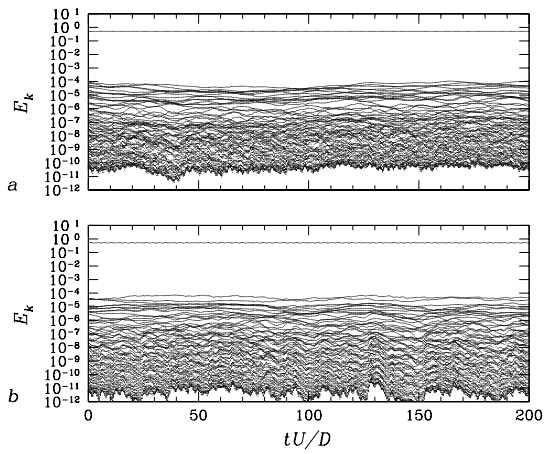

Figure 5: Time series of modal energies E_k for (a) fixed and (b) oscillating cylinder. The dominant value is for the mean flow, $E_0 \approx 0.5$, while the lower values $E_k < 1 \times 10^4$ are for the remaining modes $1 \leq k < 72$.

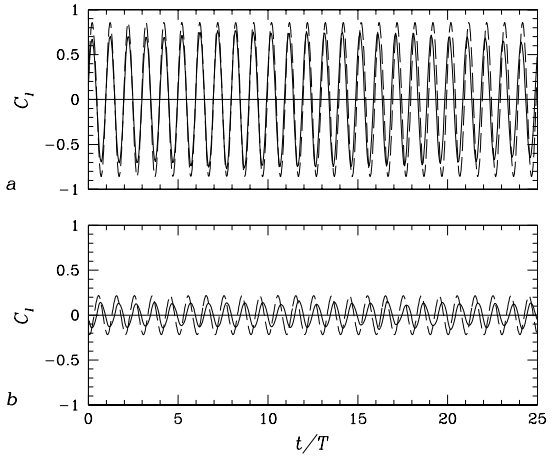

Figure 6: Time series of coefficient of lift. (a): Cylinder fixed, timebase normalised with vortex shedding period (average value in three-dimensional case). (b) Oscillating cylinder, timebase normalised with cylinder oscillation period. ——, three-dimensional flow; – –, two-dimensional flow.

In figure 6b, values of C_l for the oscillating cylinder are compared; here the timebase has been normalised using the cylinder oscillation period, and the time series are aligned such that at $t/T = 0$ the cylinder has its maximum cross-flow displacement. Again, the lower values of C_l for the three-dimensional flow in part reflects the reduced spanwise coherence of vortex shedding, but it is also apparent that the phase relationship between cylinder motion and lift force is slightly different in the two-dimensional and three-dimensional flows. This will affect the amount of mechanical work transfer between the cylinder and the flow. It is evident however that the effect of cylinder motion on lift force and phase is rather similar in the two-dimensional and three-dimensional cases.

This last point brings into question the assumption that two-dimensional and three-dimensional flows for oscillating cylinders should be compared at the same values of A and F. Rather than a pointwise comparison of this kind, it would be far more useful to have both quantitative and qualitative comparisons of behaviour over the two-dimensional (A, F) control space.

CONCLUSIONS

The results presented indicate that the imposition of cross flow cylinder motion results in the three-dimensional wake becoming more two-dimensional, but that the effect on far wake velocity correlations was greater than on the correlations of lift forces exerted on the cylinder, where the effect was comparatively small. Naturally these results must be interpreted with care, particularly by making allowance for Reynolds number effects. It remains possible however that the previously-observed increases in spanwise correlation of lift forces with motion amplitude have been less related to the effects on the inherently three-dimensional wake of an infinite circular cylinder and more with suppression of end-related perturbations in finite cylinder-length experiments.

REFERENCES

Blackburn, H. M. & Henderson, R. D. (1996). Lock-in behaviour in simulated vortex-induced vibration, *Exptl Thermal & Fluid Sci.* **12**(2): 184–189.

Blackburn, H. M. & Karniadakis, G. E. (1993). Two- and three-dimensional simulations of vortex-induced vibration of a circular cylinder, *3rd Intnl Offshore & Polar Engng Conf.*, Vol. III, Singapore, pp. 715–720.

Cantwell, B. J. & Coles, D. (1983). An experimental study of entrainment and transport in the turbulent near wake of a circular cylinder, *J. Fluid Mech.* **136**: 321–374.

Henderson, R. D. (1997). Nonlinear dynamics and pattern formation in three-dimensional wakes, *J. Fluid Mech.* **352**: 65–112.

Koopmann, G. H. (1967). The vortex wakes of vibrating cylinders at low Reynolds numbers, *J. Fluid Mech.* **28**(3): 501–512.

Novak, M. & Tanaka, H. (1975). Pressure correlations on a vibrating cylinder, *4th Intnl Conf. Wind Effects Build. & Struct.*, Cambridge University Press, Heathrow, pp. 227–232.

Williamson, C. H. K. (1989). Oblique and parallel modes of vortex shedding in the wake of a circular cylinder at low Reynolds numbers, *J. Fluid Mech.* **206**: 579–627.